IEEE Access
Multidisciplinary ⋮ Rapid Review ⋮ Open Access Journal

Received 28 October 2022, accepted 5 December 2022, date of publication 8 December 2022,
date of current version 14 December 2022.

Digital Object Identifier 10.1109/ACCESS.2022.3227648

RESEARCH ARTICLE

Analysis of Non-Uniform Accreted Ice in Overhead Power Lines Using SAP2000

ALI AJDER, (Member, IEEE)
Department of Electrical Engineering, Yildiz Technical University, 34220 Istanbul, Turkey
e-mail: aliajder@yildiz.edu.tr

ABSTRACT The design principles of overhead power lines cover the effect of external loads in the atmosphere (ice load and wind load) on the layout of power transmission systems. These additional loads are closely related to the geographical and meteorological characteristics of the land, so each country projects the additional loads on the power line design by considering its conditions. The ice load, which should be especially considered in mechanical calculations of power lines, causes forces on the conductor in the vertical direction. However, these vertical forces affect only one part of the conductor in the presence of partial ice which generally occurs due to falling some ice in the power line to the ground for any reason or directly because of meteorological events and geographical features. The analysis of partial ice load is defined as the non-uniform accreted ice problem in the related studies. This study investigates the effect of non-uniform accreted ice on the conductor curve using data from Turkey. The results obtained from the non-linear model created using SAP2000 (Structural Analysis Program) are verified with the equations in the literature. The proposed model can be used to solve other problems by changing the parameters for cases in different countries.

INDEX TERMS Audible noise, conductor curve, electric field, ice load, magnetic field, non-uniform accreted ice, overhead power lines, sag, SAP2000.

I. INTRODUCTION

Manufactured structures, especially overhead power lines that must pass through high mountains, are affected by atmospheric icing in many countries, especially Japan, Canada, England, Iceland, Finland, Hungary, Norway, Czechia, Romania, and Russia [1]. Temperature, relative humidity, wind, altitude, and land features are the main factors affecting atmospheric icing [2], [3]. The reasons for the formation and accumulation of atmospheric icing in power lines are freezing rain, wet snow, in-cloud icing events, or freezing radiation fog [4].

Atmospheric icing causes different effects on power lines depending on the weight of the ice load [5]. While light icing of overhead power lines may result in such conductor galloping and line overloading, heavy ice load may cause huge hazards such as disconnection and towers falling, which result in a blackout of the power grid [6], [7], [8].

The associate editor coordinating the review of this manuscript and approving it for publication was Siqi Bu.

NOMENCLATURE

m_c	the mass of the conductor (kg/m)
l	the span length (m)
M_i	the mass of the ice on the conductor (kg/m)
m_i	the mass of the partial ice-loaded part of the conductor (kg/m)
m	the coefficient of partial ice overload
f	the sag (m)
M	the moment (Nm)
T	the tensile force (kg)
E	young's module $\left(\text{kg/mm}^2\right)$
α	the coefficient of thermal expansion (1/°C)
q	the cross-sectional area of the conductor $\left(\text{mm}^2\right)$
θ	the temperature (°C)

It is crucial to note that, although ice load is an essential parameter to calculate mechanical stress, the overhead power lines are not only under the effect of ice load but also are affected by the wind forces, too [2]. In the project stage, the calculations are separately made for phase conductors

and protection wires, considering the conductors' weights and these extra loads [9]. These forces or loads cause the selection of larger traverses, diagonals, and perpendicular sections, which result in a cost increase for poles [10], [11]. While the loads arising from ice also include wind load, it is excluded from the scope of this study because the final state of the conductor curve is examined [12]. Therefore, it is assumed that the conductor is only affected by the ice load to create the model structure. Let the direction of two neighboring poles relative to each other is considered horizontal, and the direction of the power line relative to the ground is vertical. The sag of conductors changes only through vertical direction under uniform atmospheric icing. However, it is shifted in both horizontal and vertical directions by the effect of non-uniform accreted ice. Moreover, the probability of non-uniform accreted ice in overhead power lines that have particular importance due to the natural obstacles should be examined in detail, particularly during the project phase [13].

In studies on atmospheric icing in power transmission lines, it is generally assumed that the ice uniformly covers the conductor along the span [14]. However, the sun's rays may be partially obscured by mountains or trees, depending on the nature of the land. In this case, a portion of the ice may be melted or spilled from a hanger point, so non-uniform accreted ice may arise. The studies about non-uniform atmospheric icing in the literature are related to either the asymmetry shape of the ice over the conductors or asymmetric icing over the different phases' conductors [15]. Most studies have focused on the conductor forces and their effect on the sag [16], [17]. In other studies, the general assumption is that ice load over the sag curve is uniformly distributed [18], [19]. The calculation of unbalanced stresses under non-uniform accreted ice has been focused on only a few studies in the literature. However, studies on this subject are essential as the change of sag due to non-uniform ice directly affects the calculation of physical and electrical quantities [20], [21]. Besides, some computer programs have been developed for static loads caused by broken conductors or different ice conditions. However, these applications still need to be sufficiently tested for a general application [22], [23].

This study investigates the effect of non-uniform accreted ice on the sag for overhead lines. The displacement of the horizontal tangent point of the non-uniform accreted ice on the overhead power lines is critical as this change directly affects the magnetic coupling, electric field, magnetic field, and noise calculations which subject many studies in the literature on the surrounding pipelines [24], [25], [26], [27], [28]. The modeling and structural analysis of the overhead line is conducted using SAP2000, which is especially preferred in the solutions of non-linear problems.

II. METHODS

A. THE CHARACTERISTICS OF OVERHEAD POWER LINES

Aluminum conductor steel reinforced (ACSR), a stranded conductor with high capacity and strength, is generally used in overhead power lines (Figure 1).

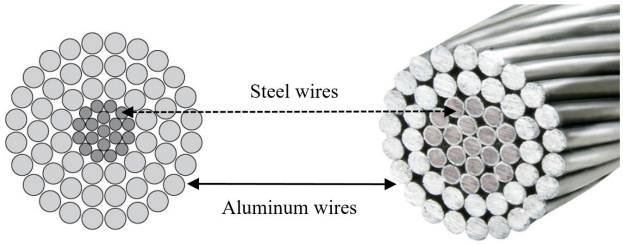

FIGURE 1. The construction of aluminum conductor steel reinforced conductor.

The Canadian Standards (CSI) use bird names (hawk, rail, cardinal...) to define the aluminum conductor steel reinforced. Therefore, ACSRs are specified with both MCM values and the bird names, like 477 MCM Hawk, 954 MCM Rail, and 954 MCM Cardinal. The conductors up to 954 MCM are generally used up to 154 kV, and conductors with higher cross-sections are used at higher voltage levels. 1 MCM or 1 kcmil, is approximately equal to 0.5067 mm^2.

Concerning the characteristics of the conductor, the following assumptions are made.

- Firstly, in terms of bending and torsion, the power line is assumed to be perfectly flexible for the length of the span.
- Secondly, the weight of the conductor is also assumed to be uniformly distributed across the span.

B. THE PROBABILITY OF NON-UNIFORM ACCRETED ICE FORMATION ON POWER LINES

Atmospheric loads on power lines are random variables. Because wind, icing, and combined wind and ice loads vary significantly in time and space, it is best to use a statistical approach for related studies and forecasts. Therefore, statistical analysis of field data for icing events is essential during the design, construction, and operation of power transmission lines, particularly for lines passing through regions with severe icing conditions [14], [29]. Ice load (kg/m), wind load (kg/m, kg/h), and iced conductor diameter thickness (mm) datasets were taken from conductor samples located in a region at specific time and time intervals (for example, at 15-minute intervals for ten years) are used in statistical studies.

The probability of non-uniform accreted ice forming on the power line can be expressed more theoretically in the following:

$$X \rightarrow \textit{is a vector random variable}$$
$$X = \begin{bmatrix} X_1 \\ \vdots \\ X_n \end{bmatrix} = [\, X_1 \quad X_2 \quad \ldots \quad X_n \,]^T \qquad (1)$$

"T" denotes the transposition of the matrix in Equation 1. Assume that the variables in Equation 1 are defined as follows:

X_1 the density of ice $\left(\mathrm{kg/m^3}\right)$
X_2 the ambient temperature (°C)
X_3 the relative humidity (%)
X_4 the wind speed acting perpendicular to the conductor (m/s)
X_5 the structure of land (Type1, Type2, ...)
X_6 the type of ice (wet − snow, in − cloudicing, ...)
X_7 the elevation from the sea level (m)
X_8 the angle of incidence of radiation to the conductor (°)

Note: $X_8 = \arccos[cos\,(113.5 - \vartheta)\,cos\,(180 - \psi)]$

ϑ the latitude of the overhead power line
ψ the angle between the line direction and the North-South direction
X_9 the intensity of solar radiation $\left(\mathrm{W/m^2}\right)$

Let $E = f(X_1, X_2, \ldots X_9)$ represent the event of formation of the non-uniform accreted ice in the power line depending on the critical factors. Suppose that the set S is the union of the mutually exclusive sets $X_1, X_2, \ldots X_9$, and the set E is a subset of S. In this assumption, S describes the set formed by all the values of critical factors, thereby E is given in the following using the set theory:

$$\begin{aligned} E &= E \cap S = E \cap \left(X_1 \cup X_2 \cup \quad \ldots \quad \cup X_9\right) \\ &= (E \cap X_1) \cup (E \cap X_2) \cup \ldots \cup (E \cap X_9) \end{aligned} \tag{2}$$

Using the law of total probability theorem in Equation 2:

$$P(E) = P(E \cap X_1) \cup P(E \cap X_2) \cup \ldots \cup P(E \cap X_9) \tag{3}$$

Using the product theorem for conditional probability in Equation 3:

$$P(E \cap X_k) = P(X_k \cap E) = P(X_k)\,P(E|X_k) \tag{4}$$

Finally, Equation 5 is obtained by writing Equation 4 explicitly:

$$\begin{aligned} P(E) = P(X_1)\,P(E|X_1) + P(X_2)\,P(E|X_2) \\ + \ldots + P(X_9)\,P(E|X_9) \end{aligned} \tag{5}$$

Complete and accurate datasets from fieldwork are needed to calculate the probability of partial ice load formation. Suppose the probability calculated using these datasets is outside the confidence interval determined previously to use in reliability studies. In that case, it is beneficial to conduct modeling and analysis, which are the subject of this study. When calculating these probabilities for regions where additional loads are severe, failure reports from previous years are also considered.

C. THEORETICAL CALCULATION OF THE DISPLACEMENT OF HORIZONTAL TANGENT POINT

Theoretical calculations are generally limited to cases where the conductor has loaded half a span or one-third of a span from the support point. However, it is crucial to evaluate the shape of the new balance curve and to check the distances of the horizontal tangent point to the ground or obstacles for the latest balance state.

Calculating the horizontal tangent point varies depending on whether it is formed on the iced or iceless part of the conductor.

If the horizontal tangent point is formed on the iceless part:

$$x = \frac{l}{2}\left[1 - \frac{(m_c + M_i) - M_i}{m_c}k^2\right] \tag{6}$$

If the horizontal tangent point is formed on the iced part:

$$x = \frac{l}{2}\left[\frac{(m_c + M_i) - m_c}{m_c + M_i}k\,(2 - k) + \frac{m_c}{m_c + M_i}\right] \tag{7}$$

The k in Equations 6 and 7 is expressed as:

$$k = \left.\frac{\textit{the length of the iced part}}{\textit{span length}}\right\} \leq 1.00 \tag{8}$$

The displacement of the horizontal tangent point due to the non-uniform accreted ice:

$$\Delta x = \frac{l}{2} - x \tag{9}$$

Considering,

$$k_0 = \frac{\sqrt{m_c\,(m_c + M_i)} - m_c}{(m_c + M_i) - m_c} \tag{10}$$

By comparing Equations 8 and 10:

If $k > k_0 \rightarrow$ the horizontal tangent point forms on the iced part of the conductor,

If $k < k_0 \rightarrow$ the horizontal tangent point forms on the iceless part of the conductor.

To theoretically present the details of calculating the sag under non-uniform accreted ice, assume that half of the conductor is subjected to partial ice load. The A and B represent the suspension points, and O shows the midpoint of the conductor, where the partial ice ends. The arc lengths OA and OB should be expressed separately to calculate the sag at point O. Then, using the properties of funicular polygons, the sag at any point of the polygon is given by,

$$f = \frac{M}{T} \tag{11}$$

M denotes the moment at the point, and T is the horizontal tensile force. The reaction forces at points A and B are given in the following, respectively.

$$R_A = m_c \frac{l}{8}\,(3m + 1) \tag{12}$$

$$R_B = m_c \frac{l}{8}\,(3 + m) \tag{13}$$

$$m = \frac{m_c + m_i}{m_c} \tag{14}$$

The moments of the reaction forces R_A and R_B are summed considering their directions to obtain the moment M at point O;

$$M = R_A \frac{l}{2} - \frac{m m_c l^2}{8} = \frac{m_c l^2}{16}\,(m + 1) \tag{15}$$

The sag at the point O is obtained by substituting the moment M in Equation 11,

$$f = \frac{m_c l^2}{16T}(m+1) \tag{16}$$

T is the tensile force at the horizontal tangent point in Equation 16. The change of state equation using the classical formulation is given in Equation 15 [30]:

$$T_2^2\left[T_2 + \frac{m_c^2 l^2 Eq}{24T_1^2} + Eq\alpha\left(\theta_2 - \theta_1\right) - T_1\right] = \frac{m_c^2 l^2 Q^2 Eq}{24} \tag{17}$$

The following results are obtained using Equation 17:

If the non-uniform accreted ice is formed on $\frac{l}{2}$ of the conductor $\rightarrow Q^2 = \frac{5m^2+6m+5}{16}$

If the non-uniform accreted ice is formed on $\frac{l}{3}$ of the conductor $\rightarrow Q^2 = \frac{3m^2+8m+16}{27}$

If the non-uniform accreted ice is formed on $\frac{2l}{3}$ of the conductor $\rightarrow Q^2 = \frac{16m^2+8m+3}{27}$

D. THE IMPLEMENTATION OF THE DEVELOPED MODEL

The forces to be applied to the power line depend on the shape of the conductor. Therefore, a non-linear analysis is required to understand the mechanical behavior of the line. As the initial geometry affects the subsequent behavior of the conductor, it is essential to model the power line correctly. In this study, it is decided to model it with one-meter intervals from the results obtained by trying different segment lengths. Figure 2 shows the conductor loading for each meter of conductor segments after defining the conductor geometry and supports for 400 meters.

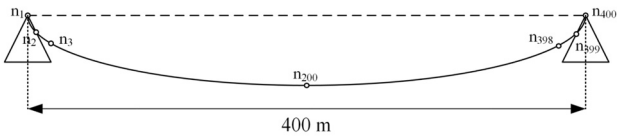

FIGURE 2. The conductor modeling approach.

Figure 3 shows the SAP2000 model of the conductor visualized above.

As seen in Figure 3, it is possible to obtain results for each joint of the conductor, which is modeled at 1-meter intervals as described above.

The flow chart of the displacement of the horizontal tangent point of the power line under non-uniform accreted ice is shown in Figure 4.

The mechanical properties of the conductor given in the Appendix vary according to the power line type to be preferred. The power transmission line specifications mean, for example, the rise difference between the two neighboring poles in a mountain or rough terrain pass. Spans in this situation are called asymmetrical (inclined) spans; greater forces load the suspension points in these cases.

The determination of the span depends on the related project. The length of the conductor pieces to be modeled is

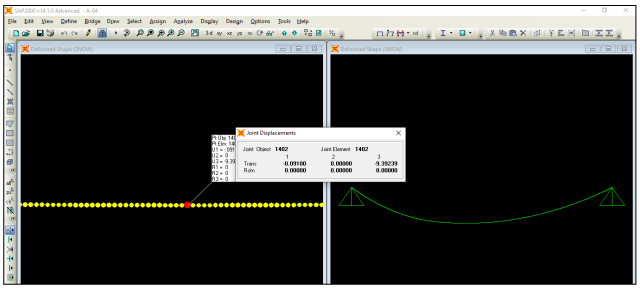

FIGURE 3. SAP2000 model of the conductor.

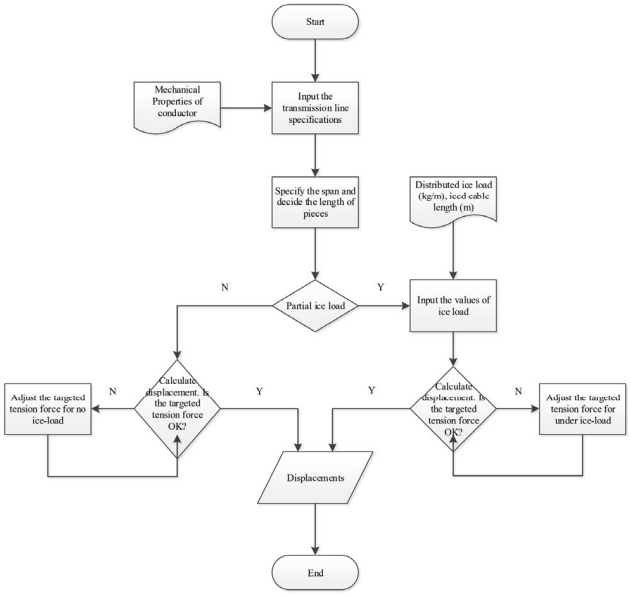

FIGURE 4. The flow chart of calculation of displacements under non-uniform accreted ice on power transmission lines.

decided according to how the resulting sensitivity is desired. Afterward, it is defined whether the power transmission line to be modeled is exposed to non-uniform accreted ice, the weight of the ice load (kg/m), and how much length of the line is affected by it. Finally, the power transmission line displacement in the horizontal and vertical directions is obtained by considering the targeted tension force.

III. NUMERICAL STUDY AND RESULTS

The presented model in this study can be applied to all power lines with different mechanical properties and non-uniform accreted ice. While deciding on the conductor type for this study, we care about its use at 420 kV and to be used more in Turkey. The only difference between Rail and Cardinal conductors, which have the same aluminum cross-section (954 MCM) and, therefore, the same electrical resistance, is that the steel core cross-sections are different. The 954 MCM Cardinal is discussed in this study's modeling part because the conductor's mechanical strength is higher than the Rail. The mechanical properties of the power transmission line to be modeled are given in the Appendix.

TABLE 1. SAP2000 windows for properties of the modeled conductor.

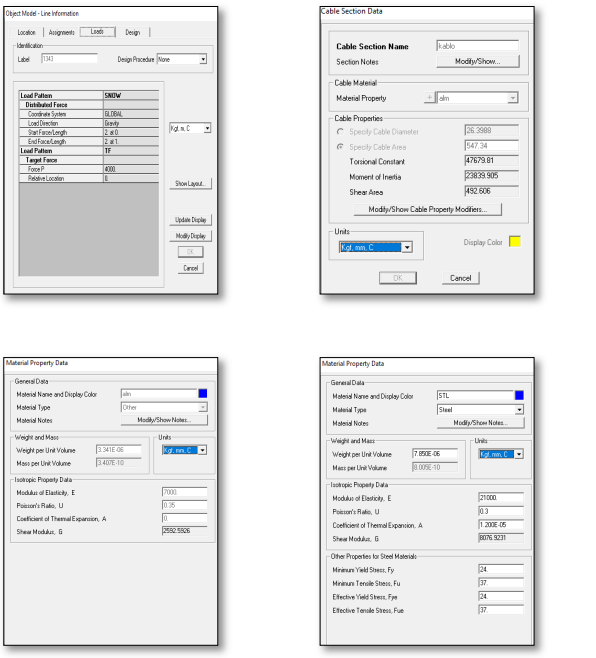

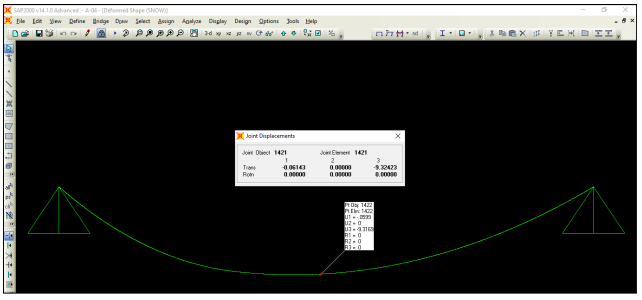

FIGURE 5. The SAP2000 main screen showing the balance and stress distribution of the conductor.

The overhead power line's tensile forces at maximum stress and maximum sag in Turkey are defined by the Turkish Electricity Transmission Company (TEIAS). The maximum tensile force for 954 MCM conductors is 4920 kg, according to the values taken from TEIAS. This value is used as a reference in the created model. The weight of non-uniform accreted ice is included in the model as 2 kg/m, assuming that it is in the III region, which is one of the regions for ice loads defined by TEIAS. The SAP2000 windows, which include the properties of the conductor in the Appendix, are given in Table 1.

The main screen of SAP2000 that shows the power transmission line's balance and stress distribution under dead load and external/snow load with the conductor simulation is given in Figure 5. These simulations are performed for each external load, and the results of different cases are obtained.

For the verification of the model created in SAP2000, the results of the presented model are compared with the well-known equations in the literature, and the results are given in Table 2 [30].

TABLE 2. Verification of the model.

Description	Formula	Sag at the end of iced-point calculated from Formula	Sag at the end of iced-point SAP2000	Sag (m) SAP2000
1/3 iced-line	$f^* = \frac{g_i a^2}{27H}\left(\frac{g_i+g_b}{g_i}+2\right)$	9.02	9.047	9.393
1/2 iced-line	$f^* = \frac{g_i a^2}{16H}\left(\frac{g_i+g_b}{g_i}+1\right)$	11.50	11.58	11.853
2/3 iced-line	$f^* = \frac{g_i a^2}{27H}\left(2\frac{g_i+g_b}{g_i}+1\right)$	11.43	11.518	13.945

It should be highlighted that these calculations can be made using these equations only if there is a certain amount of non-uniform accreted ice on the conductor. It can be seen in Table 2 that the equations give the sag at the end of the iced point. However, in many cases, especially in electrical calculations, the point where the conductor is closest to the ground is critical. Figure 6 shows the displacement of the sag according to different non-uniform accreted ice.

In Figure 6, the red line shows the location of the sag in the absence of any non-uniform accreted ice; as expected, this sag occurs in the middle of the span. It can be seen from Figure 6 that different colors show different amounts of non-uniform accreted ice in the power transmission line. The cross marks indicated in three cases show where and how much they sag through the span in the related cases. If 1/3 of the line is exposed to non-uniform accreted ice, the sag from the SAP2000 model is obtained at 178 meters of the span and 9.393 meters. If 1/2 of it is iced, the sag is calculated at 176 meters of the span and 11.853 meters; if 2/3 of the line is iced, it is obtained at 191 meters of the span and 13.945 meters.

In the second part of the study, the covered length by the 2 kg/m non-uniform accreted ice in the power transmission line is gradually increased at 40-meter intervals. As expected, the sag in case of only 40 meters of non-uniform accreted ice on the conductor is closest to the sag in the absence of ice load. The maximum horizontal displacement of the sag occurs when there are 160 meters of non-uniform accreted ice on the conductor. The SAP2000 results for this case are given in Table 3 as an example.

The U1, U2, and U3 axes considered as the reference in the modeled conductor are shown in Figure 7.

As mentioned above, in the case of uniform atmospheric icing, the modeled joints of the conductors only change in the direction of the U3 axis. In contrast, this change will be in both U1 and U3 directions with the effect of non-uniform accreted ice.

It should be noted that since no force affects the conductor in the perpendicular direction to the viewing angles of the poles, U2 values are obtained as zero in Table 3. Calculation of the displacements of each joint for the modeled conductor considering the values in Table 3 is shown in Figure 8.

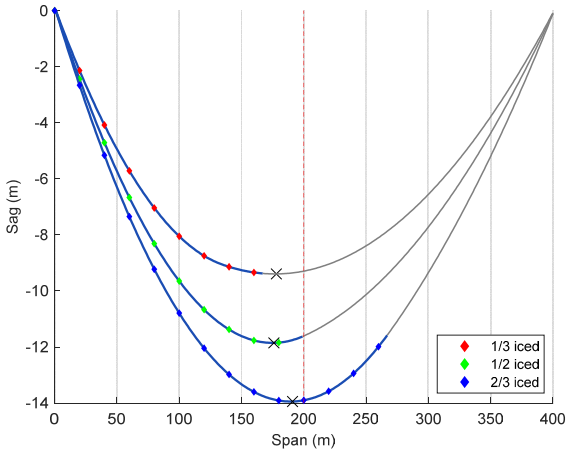

FIGURE 6. Displacement of the sag according to different non-uniform accreted ice.

TABLE 3. The SAP2000 results for a 160-meter non-uniform accreted ice in a power transmission line.

Joint	OutputCase	CaseType	StepType	U1 (m)	U2 (m)	U3 (m)
1	SNOW	NonStatic	Max	0	0	0
2	SNOW	NonStatic	Max	-0.006102	0	-0.126224
⋮	⋮	⋮	⋮	⋮	⋮	⋮
164	-	NonStatic	Max	-0.135109	0	10.327066
165	-	NonStatic	Max	-0.133274	0	10.327683
166	-	NonStatic	Max	**-0.131439**	0	**10.327926**
167	-	NonStatic	Max	-0.129604	0	10.327793
168	-	NonStatic	Max	-0.127769	0	10.327285
⋮	⋮	⋮	⋮	⋮	⋮	⋮
399	-	NonStatic	Max	0.003892	0	-0.174828
400	-	NonStatic	Max	0	0	0

The effect of the non-uniform accreted ice in the power transmission line, whose length is gradually increased on the sag, differs as stated above. This effect is analyzed by comparing the modeled minimum non-uniform accreted ice on the conductor with the maximum horizontal and vertical displacement cases. Figure 9 shows that when 40% of the conductor is iced, the sag is exposed to maximum horizontal displacement, while 90% is iced, it is exposed to maximum vertical displacement. The vertical distance of the fully ice-loaded conductor to the pipeline (observation point) occurs at midspan. However, the pipeline may only rarely be located precisely in the middle of the span. In this case, the distance of the phase conductor to the pipeline with partial ice load may take a critical value depending on the (x,y) coordinates of the two points.

The results of the sag change mentioned above are summarized in the following:

The average distance between the phase conductor and the ground is used to calculate magnetic coupling (mV), electric field (kV/m), magnetic field (mT), and noise (dB, dBA) acting on surrounding pipelines. H,H_{clamp}, *and* f denote the average distance between the phase conductor and the ground, the distance between the clamp point and the ground, and sag, respectively.

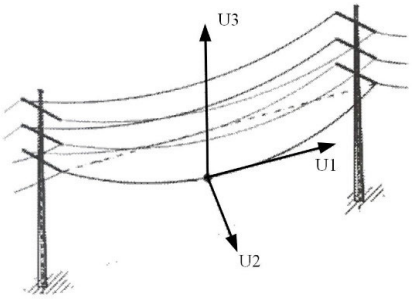

FIGURE 7. U1, U2, and U3 axis for the modeled conductor.

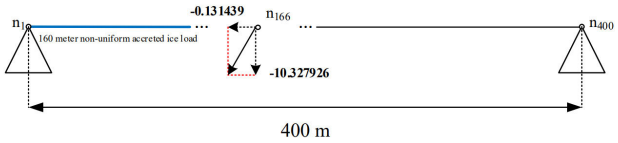

FIGURE 8. Calculation of the displacements of each joint for the simulated conductor.

In case the conductor is fully iced:

$$H = H_{clamp} - \frac{2}{3}f \quad \text{(m)} \tag{18}$$

When the non-uniform accreted ice is formed on the conductor:

$$H' \approx H_{clamp} - \frac{2}{3}f^* \quad \text{(m)} \tag{19}$$

The electric field intensity (E) is a function of the electric charge (Q), $E = f(Q)$. The relationship between the electrical charges ($Q_a\ Q_b\ Q_c$) and voltages ($V_a\ V_b\ V_c$) of phases a, b, and c is given using Maxwell's potential coefficients matrix [P].

$$[Q] = [P]^{-1}\,[V] \tag{20}$$

In a single-circuit power line, [P] is 3 × 3 dimensional, and its diagonal elements show the self-potential coefficients of phases a, b, and c.

For example, the self-potential coefficient of phase a is given by,

$$P_{aa} = \frac{1}{2\pi\epsilon_0} ln\left(\frac{2y_a}{r}\right) \tag{21}$$

r is the radius of the conductor, and y_a is the height of phase a from the ground. When the non-uniform accreted ice is formed on the conductor, y_a is rewritten by the following,

$$y_a = height\ of\ the\ pole - (height\ of\ the\ suspension\ insulator + f^*) \tag{22}$$

The magnetic flux density of the current of phase a (I_a) at the ground level through the law of Biot-Savart and Ampere is given by,

$$B_a = \frac{\mu_0 I_a}{2\pi y_a} \tag{23}$$

Hence, the magnetic field intensity changes with the variation of y_a.

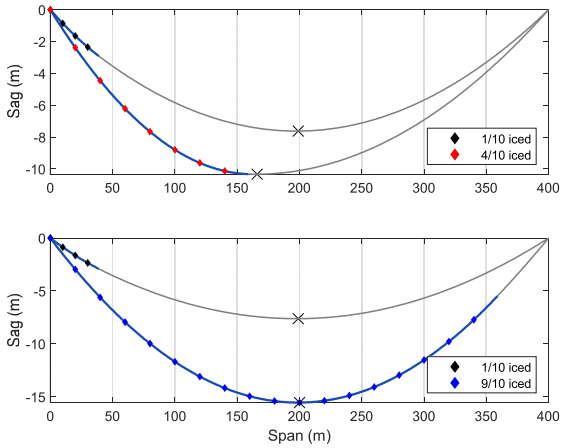

FIGURE 9. The maximum horizontal and vertical displacements cases for sag.

Various empirical formulas are determined for calculating Audible Noise (AN) caused by power transmission lines. For example, BPA (Bonneville Power Administration) defines the following empirical formulas based on the number of bundles for AC power lines with bundle conductors. AN_a, which is caused by phase a at the ground level, is presented in the following,

$$AN_a = 120log(E_a) + 55log\,(d) - 11.4log\,(y_a) - 115.4 \quad for\ n < 3 \tag{24}$$

$$AN_a = 120log(E_a) + 55log\,(d) - 11.4log\,(y_a) + 26.4log\,(n) - 128.4 \quad for\ n > 3 \tag{25}$$

In Equations 24 and 25, E_a is the maximum voltage gradient of phase a, d is the radius of the conductor, n is the number of bundles, and y_a is the distance between the center of the bundle radius of phase a and the ground. The effect of audible noise will increase when the distance of the partially iced conductor decreases from the ground (observation point). However, the numerical value of AN (dBA) depends on the meteorological parameters of the environment (especially relative humidity) and is determined by measurement in the field.

Furthermore, the following variation should also be considered where the non-uniform accreted ice is formed in the power line.

The horizontal oscillation distance (C) of the conductor changes with the effect of the wind.

In case the conductor is fully iced:

$$C = l_{in}sin\alpha_{in} + fsin\alpha_c + e \quad \text{(m)} \tag{26}$$

When the non-uniform accreted ice is formed on the conductor:

$$C' \approx l_{in}sin\alpha'_{in} + f^*sin\alpha'_c + e \quad \text{(m)} \tag{27}$$

l_{in} is the length of the suspension insulator, α_{in} is the oscillation angle of the insulator, α_c is the oscillation angle of the conductor, and e denotes the horizontal safety distance depending on the voltage.

TABLE 4. The properties of the overhead power line.

ACSR	Rated section MCM	954
	Code	Cardinal
Standard Section (mm^2)	Aluminum	484.53
	Steel	62.81
	Total	547.34
Number of layers		4
Wires in the layers		1/6/12/18/24
Aluminum	Numbers	54
	Diameter (mm)	3.38
Steel	Numbers	7
	Diameter (mm)	3.38
Standard diameter (mm)	Total conductor	30.42
	Steel core	10.14
Rated tensile stress (kgf)		15589
Unit weight (kg/km)		1829
Young's modulus (kg/mm^2)		7000
Coefficient of average thermal expansion ($1/^0C$)		19.4×10^{-6}

The minimum distance between phase conductors (D_{min}) depends on the sag.

For example, in Turkey:

$$D_{min} = 0.5\sqrt{f_{max} + l_{in}} + \frac{U}{150} \quad \text{for strain insulator } l_{in} \approx 0, \tag{28}$$

in China:

$$D_{min} = k_{in}l_{in} + \frac{U}{150} + 0.65\sqrt{f}_{max} \quad \text{for suspension insulator } k_{in} = 0.4, \quad \text{for strain insulator } k_{in} \approx 0, \tag{29}$$

f_{max} denotes the maximum sag of the conductor in Equations 28 and 29.

When the non-uniform accreted ice is formed on the conductor, it is clear $D'_{min} > D_{min}$ due to $f^* > f_{max}$.

IV. CONCLUSION AND FUTURE WORK

The effect of non-uniform accreted ice on the sag in overhead lines is described as how to conduct it on SAP2000. The sag calculations according to the different amount of ice load for overhead power line based on SAP2000 is derived and compared with the results in the literature. A 400-meter power transmission line example is selected to check the practicability and reliability of the algorithm and results. The displacement of the sag due to the non-uniform accreted ice causes changes in both physical and electrical quantities such as magnetic coupling, electric field, magnetic field, and noise. In addition, the wind load affecting the conductor exposed to non-uniform accreted ice changes due to the variation of oscillation distance of conductors. Therefore, the minimum distance calculations between phases should be considered. In addition, it is crucial to note that the non-uniform accreted ice, particularly in the protection wire, seriously affects mid-span clearance violations. This novel modeling study has practical value and will provide references for related studies.

For our future work, we plan to further scrutinize our model by applying our method with fieldwork through collaboration with TEIAS. The evidence for the formation of non-uniform

accreted ice and fault or damage caused by partial ice in the power transmission line can be accessed through a comprehensive dataset to create an accurate and effective probability model of partial ice load. In this way, we would benefit TEIAS, the power system operator in Turkey, in the reliability studies of the system. Moreover, datasets from fieldwork can be shared as open access so that other researchers can conduct further analysis and modeling studies on the subject.

APPENDIX

See Table 4.

ACKNOWLEDGMENT

Ali Ajder thanks Civil Engineer Tolga Akgul for his help in creating the cable model in SAP2000.

REFERENCES

[1] S. M. Fikke, J. E. Kristjánsson, and B. E. K. Nygaard, "Modern meteorology and atmospheric icing," in *Atmospheric Icing of Power Networks*. Dordrecht, The Netherlands, 2008, doi: 10.1007/978-1-4020-8531-4_1.

[2] M. Kermani, M. Farzaneh, and L. E. Kollar, "The effects of wind induced conductor motion on accreted atmospheric ice," *IEEE Trans. Power Del.*, vol. 28, no. 2, pp. 540–548, Apr. 2013, doi: 10.1109/TPWRD.2013.2244922.

[3] L. Chen, H. Zhang, Q. Wu, and V. Terzija, "A numerical approach for hybrid simulation of power system dynamics considering extreme icing events," *IEEE Trans. Smart Grid*, vol. 9, no. 5, pp. 5038–5046, Sep. 2018, doi: 10.1109/TSG.2017.2679109.

[4] H. Ducloux and B. E. K. Nygaard, "Ice loads on overhead lines due to freezing radiation fog events in plains," *Cold Regions Sci. Technol.*, vol. 153, pp. 120–129, Sep. 2018, doi: 10.1016/j.coldregions.2018.04.018.

[5] X. B. Huang, F. Zhang, H. Li, and X. Liu, "An online technology for measuring icing shape on conductor based on vision and force sensors," *IEEE Trans. Instrum. Meas.*, vol. 66, no. 12, pp. 3180–3189, Dec. 2017, doi: 10.1109/TIM.2017.2746438.

[6] Y. Deng, T. Xu, Y. Li, P. Feng, and Y. Jiang, "Icing thickness prediction of overhead transmission lines base on combined kernel function SVM," in *Proc. IEEE Conf. Energy Internet Energy Syst. Integr. (EI2)*, Nov. 2017, pp. 1–4, doi: 10.1109/EI2.2017.8245355.

[7] S. Lashkarbolooki, A. Pahwa, A. Tamimi, and R. Yokley, "Decreasing the ice storm risk on power conductors by sequential outages," in *Proc. North Amer. Power Symp. (NAPS)*, Sep. 2017, pp. 1–4, doi: 10.1109/NAPS.2017.8107285.

[8] L. Chen, X. Shi, B. Peng, and J. Sun, "Dynamic simulation of power systems considering transmission lines icing and insulators flashover in extreme weather," *IEEE Access*, vol. 10, pp. 39656–39664, 2022, doi: 10.1109/ACCESS.2022.3166483.

[9] C. A. Christodoulou, L. Ekonomou, A. D. Mitropoulou, V. Vita, and I. A. Stathopulos, "Surge arresters' circuit models review and their application to a hellenic 150 kV transmission line," *Simul. Model. Pract. Theory*, vol. 18, no. 6, pp. 836–849, Jun. 2010, doi: 10.1016/j.simpat.2010.01.019.

[10] J. Yu-Zhuo and L. Rui-peng, "Form-finding system for overhead transmission line based on ANSYS," *Energy Proc.*, vol. 17, pp. 975–982, Jan. 2012, doi: 10.1016/j.egypro.2012.02.196.

[11] G. He, Q. Hu, B. Wu, L. Shu, X. Jiang, L. Xiao, and Z. Yu, "Influence of freezing water conductivity on the positive corona performance of soft rime ice-covered conductor," *Int. J. Electr. Power Energy Syst.*, vol. 112, pp. 137–143, Nov. 2019, doi: 10.1016/j.ijepes.2019.04.048.

[12] Y. Huang, M. S. Virk, and X. Jiang, "Study of wind flow angle and velocity on ice accretion of transmission line composite insulators," *IEEE Access*, vol. 8, pp. 151898–151907, 2020, doi: 10.1109/ACCESS.2020.3017507.

[13] L. Al-Kanj, B. Bouzaiene-Ayari, and W. B. Powell, "A probability model for grid faults using incomplete information," *IEEE Trans. Smart Grid*, vol. 8, no. 2, pp. 956–968, Mar. 2017, doi: 10.1109/TSG.2015.2447275.

[14] J. Ranta, A. Polojärvi, and J. Tuhkuri, "Scatter and error estimates in ice loads—Results from virtual experiments," *Cold Regions Sci. Technol.*, vol. 148, pp. 1–12, Apr. 2018, doi: 10.1016/j.coldregions.2018.01.002.

[15] P. Fu, M. Farzaneh, and G. Bouchard, "Two-dimensional modelling of the ice accretion process on transmission line wires and conductors," *Cold Regions Sci. Technol.*, vol. 46, no. 2, pp. 132–146, Nov. 2006, doi: 10.1016/j.coldregions.2006.06.004.

[16] L. Guo, Y. Xie, Q. Yu, Y. You, X. Wang, and X. Li, "Displacements of tower foundations in permafrost regions along the Qinghai–Tibet power transmission line," *Cold Regions Sci. Technol.*, vol. 121, pp. 187–195, Jan. 2016, doi: 10.1016/j.coldregions.2015.07.012.

[17] Z. Wen, Q. Yu, M. Zhang, K. Xue, L. Chen, and D. Li, "Stress and deformation characteristics of transmission tower foundations in permafrost regions along the Qinghai–Tibet power transmission line," *Cold Regions Sci. Technol.*, vol. 121, pp. 214–225, Jan. 2016, doi: 10.1016/j.coldregions.2015.06.007.

[18] S. Fikke, "Meteorological data for assessing climatic loads on overhead lines. Report from Cigré WG B2.28," in *Proc. Int. Workshop Atmos. Icing Struct. (IWAIS)*, Uppsala, Sweden, 2015, pp. 129–131.

[19] M. Cai, B. Yan, X. Lu, and L. Zhou, "Numerical simulation of aerodynamic coefficients of iced-quad bundle conductors," *IEEE Trans. Power Del.*, vol. 30, no. 4, pp. 1669–1676, Aug. 2015, doi: 10.1109/TPWRD.2015.2417890.

[20] W. Zhou, X. Zhang, X. Li, and Y. Jiang, "Computational analysis on unbalanced tension in overhead power lines under non-uniform accreted ice," *Electr. Power Syst. Res.*, vol. 202, Jan. 2022, Art. no. 107606, doi: 10.1016/j.epsr.2021.107606.

[21] R. Sopper, C. Daley, B. Colbourne, and S. Bruneau, "The influence of water, snow and granular ice on ice failure processes, ice load magnitude and process pressure," *Cold Regions Sci. Technol.*, vol. 139, pp. 51–64, Jul. 2017, doi: 10.1016/j.coldregions.2017.04.006.

[22] J. Lummis and K. E. Lindsey, "Computer-aided design of longitudinal loads on flexibility supported transmission lines," in *Proc. IEEE Power Eng. Soc., Summer Meeting Energy Resour. Conf.*, Anaheim, CA, USA, 1974, Paper C74-388-5.

[23] D. B. Campbell, "Unbalanced tensions in transmission lines," *J. Struct. Division*, vol. 96, no. 10, pp. 2189–2207, Oct. 1970.

[24] A. Alihodzic, A. Mujezinovic, and E. Turajlic, "Electric and magnetic field estimation under overhead transmission lines using artificial neural networks," *IEEE Access*, vol. 9, pp. 105876–105891, 2021, doi: 10.1109/ACCESS.2021.3099760.

[25] A. Z. E. Dein, O. E. Gouda, M. Lehtonen, and M. M. F. Darwish, "Mitigation of the electric and magnetic fields of 500-kV overhead transmission lines," *IEEE Access*, vol. 10, pp. 33900–33908, 2022, doi: 10.1109/ACCESS.2022.3161932.

[26] J. Wang and L. Gao, "Research on the algorithm and test of transmission line voltage measurement based on electric field integral method," *IEEE Access*, vol. 6, pp. 72766–72773, 2018, doi: 10.1109/ACCESS.2018.2880309.

[27] I. Kurniawan, S. Harjo, O. Pischler, and U. Schichler, "Audible noise calculation for different overhead transmission lines," in *Proc. 53rd Int. Univ. Power Eng. Conf. (UPEC)*, Sep. 2018, pp. 1–6, doi: 10.1109/UPEC.2018.8542082.

[28] *IEEE Standard for the Measurement of Audible Noise From Overhead Transmission Lines*, IEEE Standard 656-2018, 2018.

[29] M. Farzaneh, *Atmospheric Icing of Power Networks*. Chicoutimi, Canada: Springer, 2008, ch. 2, pp. 31–80.

[30] C. Avril, *Construction des Lignes Aériennes à Haute Tension: Technique Française d'études et de Réalisation*. Paris, France: Eyrolles, 1974, ch. 4, sec. 4, pp. 96–118.

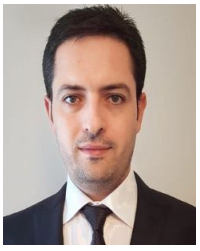

ALI AJDER (Member, IEEE) received the B.Sc. degree from the Department of Electrical Engineering, Yildiz Technical University (YTU), Turkey, in 2008, the Double Major degree from the Department of Business Administration, YTU, in 2009, and the M.Sc. and Ph.D. degrees in power systems from the Graduate School of Science and Engineering, YTU, in 2011 and 2017, respectively.

He studied at the Technische Universität Kaiserslautern, Germany, in 2006 and 2007. He is currently a Research Assistant with the Department of Electrical Engineering, YTU. His current research interests include energy economy, renewable energy, and power systems.